

Process-based modeling of morphodynamics of a tidal inlet system

XIE Dongfeng^{1,2}, GAO Shu^{2*}, PAN Cunhong¹

¹ Zhejiang Institute of Estuaries and Hydraulics, Hangzhou 310020, China

² Ministry of Education Key Laboratory for Coast and Island Development, Nanjing University, Nanjing 210093, China

Received 13 September 2010; accepted 18 October 2010

©The Chinese Society of Oceanography and Springer-Verlag Berlin Heidelberg 2010

Abstract

The morphodynamic evolution of an idealized inlet system is investigated using a 2-D depth-averaged process-based model, incorporating the hydrodynamic equations, Englund-Hansen's sediment transport formula and the mass conservation equation. The model has a fixed geometry, impermeable boundaries and uniform sediment grain size, and driven by shore-parallel tidal elevations. The results show that the model reproduces major elements of the inlet system, i.e., flood and ebb tidal deltas, inlet channel. Equilibrium is reached after several years when the residual transport gradually decreases and eventually diminishes. At equilibrium, the flow field characteristics and morphological patterns agree with the schematized models proposed by O'Brien (1969) and Hayes (1980). The modeled minimum cross-sectional entrance area of the tidal inlet system is comparable with that calculated with the statistical P-A relationship for tidal inlets along the East China Sea coast. The morphological evolution of the inlet system is controlled by a negative feedback between hydrodynamics, sediment transport and bathymetric changes. The evolution rates decrease exponentially with time, i.e., the system develops rapidly at an early stage while it slows down at later stages. Temporal changes in hydrodynamics occur in the system; for example, the flood velocity decreases while its duration increases, which weakens the flood domination patterns. The formation of the multi-channel system in the tidal basin can be divided into two stages; at the first stage the flood delta is formed and the water depth is reduced, and at the second stage the flood is dissected by a number of tidal channels in which the water depth increases in response to tidal scour.

Key words: tidal inlet, morphological evolution, sediment dynamics, numerical modeling

1 Introduction

A large part of the world's inhabited coastlines is formed by sequences of tidal inlets. A tidal inlet system is a long and narrow branch of the open sea penetrating into land, consisting of a tidal basin, one or more entrance channels, and flood and ebb tidal deltas (Ren and Zhang, 1985; Bruun, 1978). Through the entrance channels, tidally-induced water and sediment exchange between the tidal basin and the open-sea occurs. Such channels often serve as a natural navigation channel, which is important for harbors. From the viewpoint of morphodynamics, tidal inlets are interesting because their formation and evolution are concerned with a number of crucial dynamic processes.

Numerous methods can be found in the literature to study the physical processes and the long-term behavior of tidal inlets. Empirical relationships show that equilibrium exists for different morphological parameters: inlet cross-sectional area and basin tidal prism (Zhang, 1995a; Gao, 1988; Zhang, 1987; Jarret, 1976; O'Brien, 1969), inlet cross-sectional area and discharge (Kraus, 1998) and ebb-tidal delta volume and basin tidal prism (Walton and Adams, 1976), and the ratios of shoal volume to channel volume and tidal amplitude to mean channel depth (Wang et al., 1999). Recently, analytical approaches to defining tidal inlet parameters have shown that morphodynamic behaviors of tidal inlets are related to the factors such as flood and ebb durations, freshwater discharges and

Foundation item: The National Natural Science Foundation of China under contract Nos 41006053 and 40576023; the Ministry of Water Resources' Special Funds for Scientific Research on Public Causes under contract No. 201001072; the Program for Innovative Research Team of Zhejiang Province under contract No. 2009F20024.

*Corresponding author, E-mail: shugao@nju.edu.cn

sediment transport through the entrance, in addition to tidal prism (Jia and Gao, 2008; Gao and Collins, 1994).

Quantitative researches on tidal inlet evolutions have conducted to a large extent in the last decade (e.g. Bertin et al., 2004; Stive and Wang, 2003; Vila-Concejo et al., 2003; Zhang et al., 1995; Zhang, 1995b). The evolution of the entrance channels is related with the general characteristics of the tidal inlet system. Further, the hydrodynamics of tidal inlets is complex, although their spatial scales are relatively small. Recently, the mid- or small- scale flow field around tidal inlets has been studied by many researchers (e.g. Gong et al., 2009; Guyondet and Koutitonsky, 2008; Gong et al., 2008; Eguiluz and Wong, 2005; Li, 2002; Van Leeuwen and De Swart, 2002), providing abundant information on spatial distributions of current velocities, residual currents and the structure of circulation patterns within the channels. However, most studies treated the bathymetry of tidal inlets as unchangeable boundary conditions; and few focused on the feedback processes between hydrodynamics and bathymetry.

Even there is a lack of long-term (i.e., years to decades, the typical timescale of coastal morphological changes) data, developing a process-based morphodynamic model would be an important attempt to understanding the physical processes around tidal inlets. With the development of computer capacity, process-based models have been increasingly employed for coastal morphodynamic studies, such as estuaries, embayment and tidal channels (e.g. Xie et al., 2009; Xie et al., 2008; Hibma et al., 2004; Lanzoni and Seminara, 2002; Ranasinghe and Pattiaratchi, 1999; Wang et al., 1995). These models are based on physical principles, capable of simulating various morphodynamic processes of hydrodynamics, sediment transport and seabed evolution by solving mathematical equations (De Vriend et al., 1993). Several idealized models have been used to simulate the formation and equilibrium of ebb-tidal deltas (Van der Vegt et al., 2006; Van Leeuwen et al., 2003) and the influence of tidal currents on the asymmetry of tidal-dominated ebb-tidal deltas (Van der Vegt et al., 2009), improving the understanding of underlying physical mechanisms responding for the ebb tidal deltas evolutions. The components of tidal inlet systems, such as tidal basin, entrance channel and flood and ebb deltas, interact with each other and respond to inherent or external forcing (e.g. Kragtwijk et al., 2004; Hayes,

1980; Bruun, 1978). This motivates the present study to model morphodynamics of tidal inlet systems by considering ebb delta as well as the tidal basin, main channel and flood deltas. The overall objective of the present study is to improve the knowledge of the physical mechanisms controlling the morphodynamic development of tidal inlets, focusing on tide-dominated tidal inlets floored with sandy sediments.

2 Model description

The process-based model is set up based on the state-of-art Delft3D Online Morphology modeling system (edition 3.28), in which hydrodynamics and sediment transport processes are included and for each time step the bathymetry is updated using sediment mass balance (Roelvink and Van Banning, 1994). The principal constituents of the morphodynamic model are the flow, sediment transport and bottom change modules, as described below.

2.1 Flow

The flow module computes unsteady flow resulting from tidal and meteorological forcing, based on the 2-D depth-averaged shallow water equations. The equations for conservation of momentum are

$$\frac{\partial u}{\partial t} + u \frac{\partial u}{\partial x} + v \frac{\partial u}{\partial y} + g \frac{\partial \eta}{\partial x} - fv + \frac{gu |U|}{C^2(d+\eta)} - v_w \left(\frac{\partial^2 u}{\partial x^2} + \frac{\partial^2 u}{\partial y^2} \right) = 0, \quad (1)$$

$$\frac{\partial v}{\partial t} + u \frac{\partial v}{\partial x} + v \frac{\partial v}{\partial y} + g \frac{\partial \eta}{\partial y} - fu + \frac{gv |U|}{C^2(d+\eta)} - v_w \left(\frac{\partial^2 v}{\partial x^2} + \frac{\partial^2 v}{\partial y^2} \right) = 0, \quad (2)$$

and the continuity equation is

$$\frac{\partial \eta}{\partial t} + \frac{\partial(d+\eta)u}{\partial x} + \frac{\partial(d+\eta)v}{\partial y} = 0, \quad (3)$$

where C is Chézy's friction coefficient, defined by $\frac{g\bar{d}}{n}$ ($\text{m}^{1/2}/\text{s}$), in which n is Manning's coefficient ($\text{s}/\text{m}^{1/3}$), d is water depth (m), η is water level (m), U is magnitude of total velocity (m/s), $U = \sqrt{(u^2 + v^2)}$, u and v are depth-averaged velocities in the x - and y - directions (m/s), g is gravitational acceleration (m^2/s), v_w is diffusion coefficient (m^2/s), f is Coriolis factor ($1/\text{s}$). Delft3D deals with moving boundaries by wetting/drying method (Lessor et al., 2004).

2.2 Sediment transport

Various formulae are available for sediment transport calculation in literature. Hibma et al. (2004)

tested the sensitivity of estuarine morphodynamics for different sediment transport formulae, e.g. the total-load transport formula of Engelund and Hansen (1976) and the transport formula of Van Rijn (1984) which calculated bed load transport and the equilibrium suspended sediment transport rate. Their results show that the estuarine morphodynamic development is largely analogous, with few local differences. Furthermore, Lanzoni and Seminara (2002) analyzed dominant sediment transport processes in tidal environments, with the situations of the presence of multiple sediment fractions, tidally-induced time-velocity asymmetry, continuously changing suspended sediment concentration profiles, and erosion and settling lags around slack tide. Their analysis shows that the formulae for the bed and suspended load transports based on local and instantaneous flow conditions are applicable.

Lanzoni and Seminara (2002) suggested that a relatively simple transport equation without making distinction between suspended load and bed load be used so that the results can be analyzed in a more straightforward way. This method is adopted in the present study. The instantaneous total sediment transport formula developed by Engelund and Hansen (1967) that relates velocity directly and locally to a sediment transport is used:

$$S = S_b + S_s = \frac{0.05U^5}{g^{0.5}C^3\Delta^2d_{50}}, \quad (4)$$

where S_b and S_s are bed-load and suspended sediment transport rates, respectively [$m^3/(m \cdot s)$], Δ is relative density $\frac{\rho_s - \rho_w}{\rho_w}$, ρ_s is density of sediment (kg/m^3), ρ_w is density of water (kg/m^3), d_{50} is mean sediment grain size (m).

2.3 Bed level change

Conservation of sediment is described by the following equation representing a balance between the divergence of the sediment transport field and the evolution of the bed level corrected for bed porosity:

$$(1 - \varepsilon) \frac{\partial Z_b}{\partial t} + \frac{\partial q_x}{\partial x} + \frac{\partial q_y}{\partial y} = 0, \quad (5)$$

where ε is bed porosity, default 0.4, Z_b is bed level (m), q_x and q_y are sediment transports in x - and y -directions [$m^3/(m \cdot s)$]. Bed level change is updated every time step synchronously with hydrodynamics in the state-of-art online version of Delft3D.

Tidal hydrodynamic behavior in estuaries has a

timescale that is typically one to two orders of magnitude smaller than the morphological timescale (Wang et al., 1995). In terms of numerical modeling this implies that many hydrodynamic calculations need to be performed that have only limited effect on the morphology. Morphodynamic calculations would therefore require long and inefficient hydrodynamic calculation time. In order to increase the efficiency of process-based morphodynamic models, Roelvink (2006) proposed the “online morphology” approach to accelerate bed level changes. In this approach the bed level is updated at each computational time step by multiplying the erosion and deposition fluxes from the bed to the flow and vice versa by a constant factor “Morphological Factor”

$$\Delta t_{morphology} = f_{Mor} \Delta t_{hydrodynamics}. \quad (6)$$

The morphodynamics update scheme is presented in Fig.1.

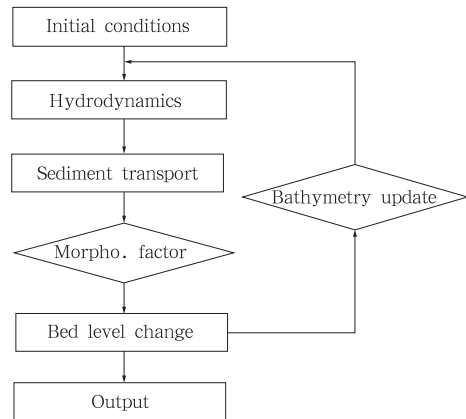


Fig.1. Morphological update scheme.

2.4 Model set-up

As compared with many tidal inlets along American or European coast that characterized by seasonal opening and closure, most tidal inlets along China’s coast are characterized with stable barriers due to their high resistance for erosion of the sediments (Zhang et al., 1995). Hence, the present model was given a fixed geometry and impermeable boundaries. For tidal inlets along China’s coast, the size of the tidal basin normally varies between 10^0 and 10^2 km^2 , with widths at the entrance being of the order of 10^2 – 10^3 m and water depths of 10^1 m. Thus, both of the inlet length and width are set to be 1 km, and the basin dimensions are assumed to be 4 km×5 km, with a flat bottom of 2 m depth (Fig. 2). Over the coastal

waters the depth is specified 2 m along the shoreline down to 20 m along the open boundary in 15 km distance. The open boundaries are located far from the inlet system such that the influences of boundary conditions on the tidal inlet is minimized. The model is forced by M_2 tide with a 1 m tidal amplitude (a typical value for the southern China coastlines). The tidal wave is set to propagate in the north-south direction. The cell size is around $100\text{ m} \times 100\text{ m}$, locally refined to be $30\text{ m} \times 30\text{ m}$ around the entrance. Time step is set to be 30 s, following the CFL criterion (Fletcher, 1988). Sediment in the tidal inlet is assumed to be uniform sand with grain size of 0.2 mm. Waves and Coriolis-effect are neglected. This model thereby simulates a tide-dominated basin that falls in the meso-tidal category of Hayes (1975). The sediment transport calculation and bed level change update are started when the flow field becomes steady, until the tidal inlet system become stable morphologically. Two observation sites, O_1 and O_2 , and one observed cross-section A are set for model result analysis, located at entrance channel and in the basin (Fig. 2).

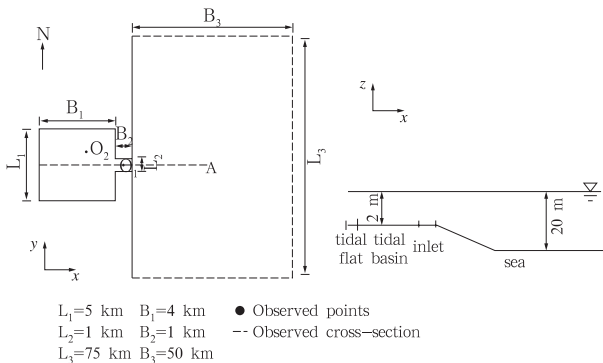


Fig.2. Configuration of an idealized tidal inlet system and the initial depth (Dashed lines represent open boundaries and dotted line represents the observed line).

In the “online” approach for the morphodynamic update, model results are valid as long as bed level changes after a time step remain small compared to the water depth (Roelvink, 2006). Sensitivity analysis is carried out by applying different morphological factors (5, 10, 20, 50, 100). The results show that the bed level updates are in the range of 1%–5% of the local water depth. However, there are points which rarely exceed this range. One morphological factor (20) is selected for this study based on the percentage of bed level update, the computational time and the required accuracy.

2.5 Morphodynamic equilibrium condition

One important issue of coastal morphological evolution is whether or not a coastal system will reach morphodynamic equilibrium (Gao and Collins, 1998). The morphodynamic equilibrium solutions of the model obey the condition ,

$$\int_0^T dqdt = 0, \quad (7)$$

which implies that gradients of sediment transport rates of every two neighboring points approach zero [cf. Eq. (5)]. In the present study, we assume that equilibrium is reached when the gradients of sediment transport rates of all neighboring points become smaller than an infinitesimal value. Generally, sediment transport rate in coastal environments is of the order of 10^{-2} – $10^{-4}\text{ m}^3/(\text{m}\cdot\text{s})$ (Van Rijn, 1993); hence, the infinitesimal value is defined to be $10^{-6}\text{ m}^3/(\text{m}\cdot\text{s})$.

3 Model results

3.1 Initial patterns

The short-term simulation results are used to understand the hydrodynamic and sediment transport characteristics. For this, we compute the tidal levels, tidal currents, residual sediment transport and erosion and deposition patterns at the initial stage.

Figure 3 shows flood and ebb maxima, residual sediment transport, erosion and deposition fluxes over one tidal cycle of the tidal inlet system at the initial stage. On the seaside, tidal currents propagate in south-north direction driven by tide wave of 1 m amplitude. Around the entrance, flood and ebb currents flow into and out the basin. The current velocities are in the order of 1 m/s, consistent with those of real inlets (e.g. Jia et al., 2003; Vila-Concejo et al., 2003; Bruun, 1978). Currents velocities vary spatially and appear largest in the restricted entrance channel. On the flood tide, currents converge from all seaward directions towards the entrance. The currents exist seaward of the entrance during the ebb tide; here, the momentum of the flow through the entrance forms a jet directed seaward. This flow patterns are consistent with the schematized current diagram of tidal inlets by O’ Brien (1969).

A major factor in understanding sediment transport processes in tidal inlets is linked to the non-linearity that determine flood or ebb dominance. Figure 4 illustrates velocity-time curves at observed point

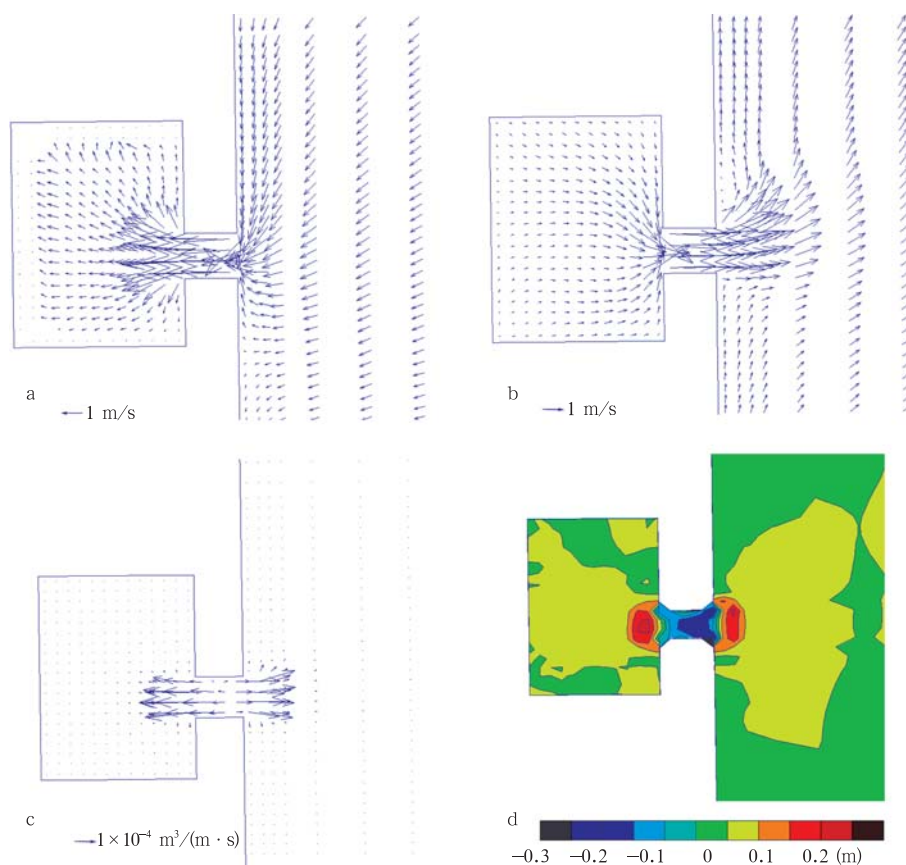


Fig.3. Flood and ebb maxima, net sediment flux and mean erosion/deposition at the bed at the initial state.

O_1 at the entrance. At initial state, tidal currents are flood dominated. The maximal flood velocity is 1.6 m/s and flood duration is 5h39m while the maximal ebb velocity is 1.2 m/s and ebb duration is 6h51m. The tidal asymmetry means that sediment transport towards the basin is more intense than seaward transport (Fig. 3c). Residual sediment transport is in the order of $10^{-4} \text{ m}^3/(\text{m}\cdot\text{s})$, with erosion and deposition mainly occurring around the entrance. The channel is excavated and the eroded sediments are deposited to the adjacent area. The eroded depth at the entrance and deposited depth in the adjacent areas are 0.25 m/s and 0.15 m/s, respectively (Fig. 3d).

3.2 Long-term simulations

Figures 5 and 6 illustrate the morphodynamic processes of the tidal inlet and the cross-section A, respectively. At the initial stage, the bed levels change rapidly. The sediment in the entrance is transported into the basin and towards the sea. After 2 months, the embryo of flood and ebb deltas can be detected. The ebb delta consists of a terminal sand lobe which is flanked on either side by marginal flood-dominated

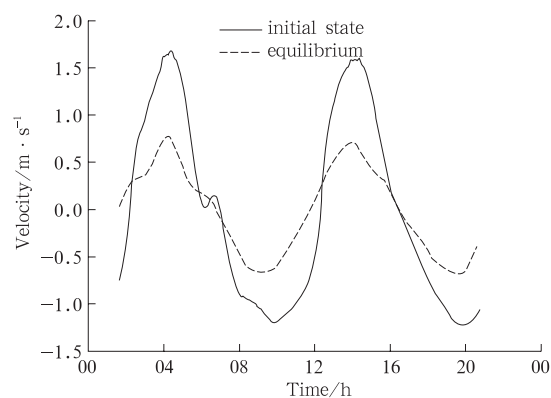


Fig.4. The velocity-time curves of observed O_1 at initial state and equilibrium.

channel. This scenario is in agreement with the morphology model of ebb-tidal deltas proposed by Hayes (1980). In response to the sediment input, the basin become shallower and the flood delta is enlarged gradually. After some 1.5 a, the flood delta is divided into several parts by tidal channels, namely, a multi-channel system is developed in the tidal basin. Meanwhile, the ebb delta moves seaward and deepens gradually. This is probably because the ebb currents erode

the ebb delta and there is no sediment source compensation, as assumed in the present model. After around 6 a, the bed level changes become negligible, and the residual sediment transport decreases to the order of 10^{-6} kg/(m·s). According to the equilibrium criterion used in the modeling, this represents an equilibrium state. Under equilibrium, the maximal water depth in the entrance is 4.8 m and the minimal depth at flood and ebb deltas are 0.8 and 1.7 m, respectively (Fig. 6). Apparently, when the morphology becomes stable, the routes of tidal currents and sediment transport are influenced by the seabed morphology and bathymetry

(Fig. 7c).

In general, the evolution rate of tidal inlet tends to slow down with time exponentially. This is consistent with previous researches (e.g. Xie et al., 2009; Van der wegen and Roelvink, 2008; Xie et al., 2008; Hibma et al., 2004). The time scale for the tidal inlet to reach equilibrium is several years, two to three orders shorter than those of estuaries and open-sea tidal channels, which is hundreds to thousands years. This may be attributed to the small spatial scale, relatively large sediment input and high energy level used in the modeling.

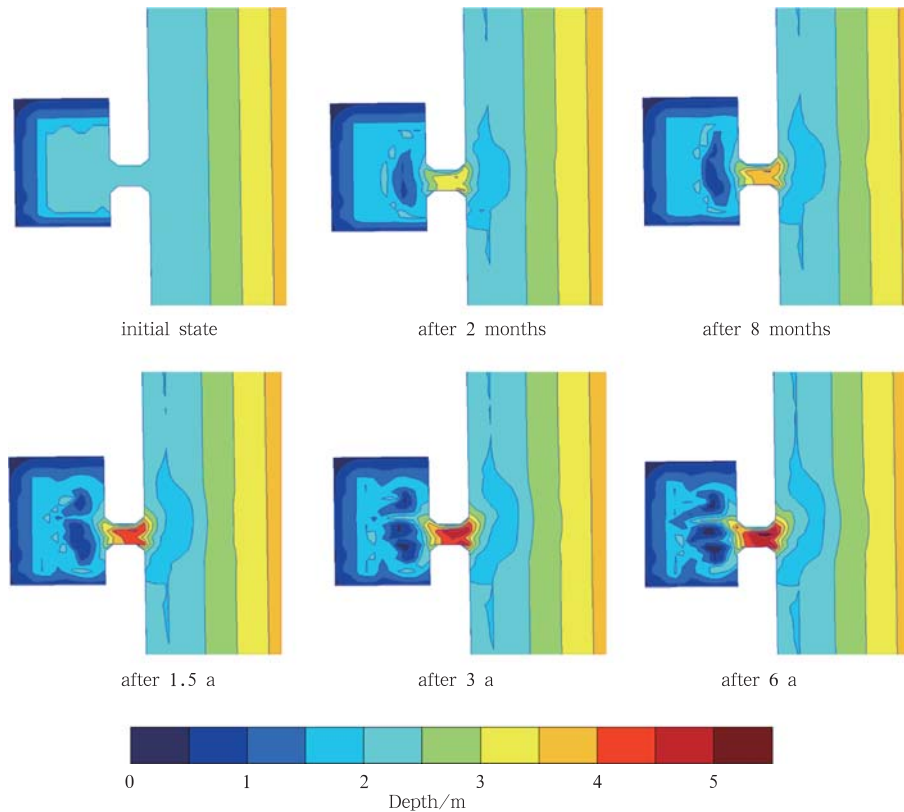


Fig.5. Morphodynamic processes of tidal inlet system formation.

The magnitude of tidal prism and the minimum cross-sectional area at the entrance channel are important parameters for characterizing tidal inlets. O'Brien (1931) proposed that there exists a power relationship between tidal prism and the cross-sectional area:

$$A = cP^n, \quad (8)$$

where A is the cross-sectional area below mean sea level (m^2), P is tidal prism (m^3), and c and n are constants. For instance, the P-A relationship for natural tidal inlets along the East China Sea coast (Gao, 1988)

read as

$$A = 2.55 \times 10^{-4} P^{0.92}. \quad (9)$$

Despite the discrepancy between natural environments along the East China Sea coast, where tidal amplitudes varies around 2 m, and sediment are mainly composed of mud and silt (e.g. ECCHE, 1992), and the above-mentioned input parameters in the current model, Eq. (9) could be used to validate the model roughly, because the underlying physical mechanisms are consistent. Figure 8 shows that the modeled min-

imum cross section area varies through time exponentially and approaches continuously to the equilibrium minimum cross section area calculated by Eq. (9)

$$A = 1\,714.6 \times t^{0.1021}, \quad (10)$$

where t is time in year. The correlation coefficient is $R^2=0.9919$. At equilibrium the minimum cross-sectional area is consistent with that calculated by Eq. (9), confirming the validity of the model results.

3.3 Feedback among hydrodynamics, sediment transport and bed level changes

There exist non-linear interactions among tidal currents, sediment transport and bed level changes. Erosion or accretion intensity of tidal inlets is related to sediment transport which, in turn, is affected by current velocities and flood/ebb durations. Take the

observation site O_1 as an example: the current velocity near the seabed is relatively large at the initial stage,

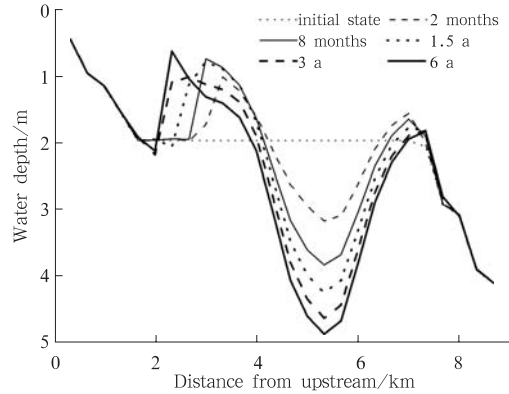


Fig.6. Water depth changes along the observed cross section A.

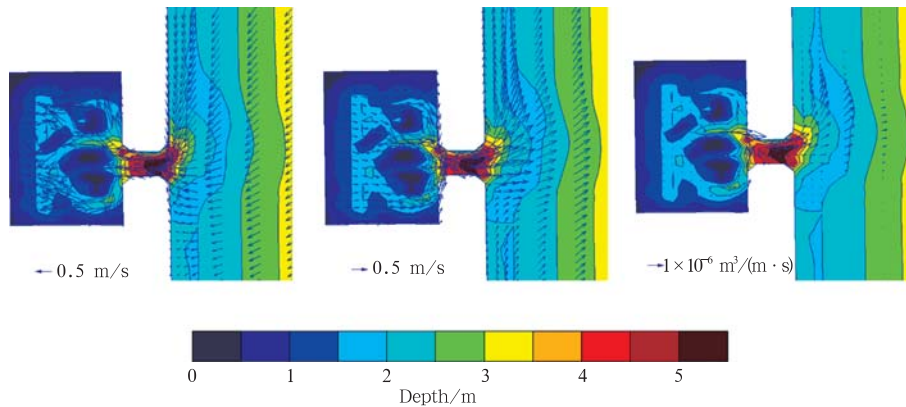


Fig.7. Flood and ebb maxima, net sediment flux at equilibrium state.

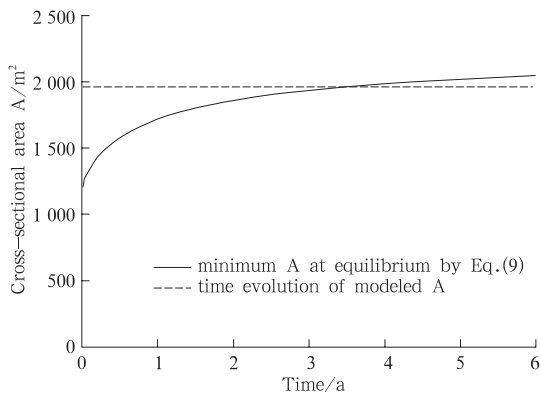


Fig.8. Changes of minimum cross section area at the entrance channel with time.

due to the shallow water depth. Consequently, sediment is transported intensively and the bed is eroded rapidly. As the water depth increases, the flood and ebb velocities decrease gradually, with maxima being

reduced from 1.60 and 1.20 m/s at initial state to 0.71 and 0.69 m/s at the equilibrium, respectively. Meanwhile, flood duration becomes 15 min longer while ebb duration shortens by 36 min. The flood dominance at O_1 decreases with morphological evolution. Ratios of maximal flood and ebb velocities decrease from 1.33 at initial stage to 1.03 at equilibrium (Table 1). As a result, net sediment transport over one tidal cycle is reduced from the order of 10^{-4} kg/(m·s) to 10^{-6} kg/(m·s).

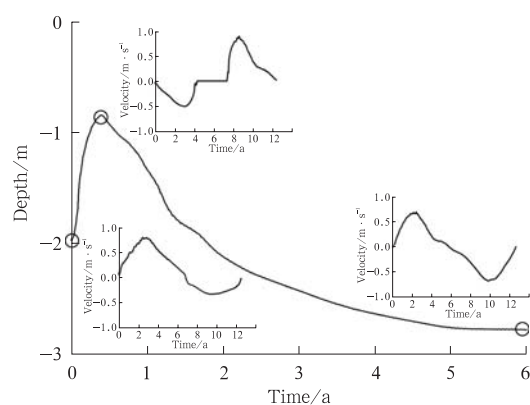
3.4 Mechanisms for multi-channel system formation

At equilibrium, the modeled flood delta is composed of several parts, which are divided by tidal channels. To identify the formation mechanism of the multi-channel system, the results from the observation site O_2 , located in one of the tidal channels between two lobes of the flood delta, are analyzed. Figure 9

Table 1. Flood and ebb durations and their maximal velocities at station O₁ at initial state and equilibrium

		Duration	Maximal current velocity/m·s ⁻¹	Ratios between maximal flood and ebb velocities
Initial state	Flood	5h39m	1.60	1.33
	Ebb	6h51m	1.20	
Equilibrium	Flood	5h54m	0.71	1.03
	Ebb	6h15m	0.69	

illustrates changes of bed level and current velocity with time. The bed level change can be divided into two stages: (1) the first 0.5 years, when the flood delta was formed and enlarged gradually, and the water depth at O₂ decreased from 2 to 0.8 m; and (2) the flood delta was divided into several parts and the channels between deltas deepened gradually, and the water depth at O₂ changed from 0.8 to 2.7 m. At the first stage, with the water depth decreased, current velocity increased accordingly. Maximum flood and ebb velocities increased from 0.8 and 0.38 m/s to 1.0 and 0.5 m/s, respectively. Once current shear stress exceeded the threshold to mobilize the sediment, the bed is eroded. With the channels deepening, flood velocity was decreased. At O₂, maximum flood velocity decreased from 1.0 to 0.7 m/s. On the other hand, ebb velocity increased because more ebb currents flow seaward through the channels after the channels were opened. At O₂, maximal ebb velocity increased from 0.5 to 0.7 m/s.

**Fig.9.** Water depth changes with time and corresponding velocity-time curves at observed point O₂.

4 Discussion

In this study, a long-term process-based morphodynamic model for an idealized tidal inlet system has been established. The model bridges the gap between short-term hydrodynamics, sediment transport and long-term morphological evolution. It can describe the changes of hydrodynamics, sediment transport and

bathymetry at various stages of the morphological evolution. When only tidal currents are taken into account, the tidal inlet system will reach morphodynamic equilibrium, and the response time is of the order of several years. This result is consistent with field observations. For example, observation at the Ancao Inlet in Southern Portugal reveals that the channel and deltas were fully developed again and translated to a new “mature” stage after only two years of its artificial opening (Vila-Concejo et al., 2003).

As pointed out by previous studies (e.g. Xie et al., 2009; Xie et al., 2008; Hibma et al., 2004; Lanzoni and Seminara, 2002; Ranasinghe and Pattiaratchi, 1999; Wang et al., 1995), negative feedback mechanisms exist between flow and bathymetry, which are responsible for the morphological evolutions of coastal system. Converging flood currents and jetting ebb currents are the main hydrodynamic mechanism for the formation of the entrance channel, and flood and ebb deltas of the tidal inlet. Flow currents cause seabed erosion and deposition which, in return, influences current velocities and durations. The system tends to evolve towards morphodynamic equilibrium by adjusting water depth, flood and ebb current velocities and durations. Sediment transport is the central process in morphodynamic evolution which links flow currents and morphological changes. Since sediment transport rate is a high-order function of current velocity (e.g. Van Rijn, 1993), the residual sediment transport decrease gradually with the system adjustment until equilibrium is reached.

Van der Vegt et al. (2009, 2006) reproduced the formation and evolution of ebb tidal delta using an idealized process-based model. Their results reveal that the morphological asymmetry of the delta depends on the magnitude of the cross-shore and large scale along-shore tidal currents and their phase difference. Their conclusions are applicable to the results of this study: the asymmetry of the modeled ebb delta with regard to the axis of the entrance is caused by the angle between current velocities around the entrance and the long-shore direction. A fully symmetric ebb delta would be related to an absolute shore-normal flow field using

Neumann conditions on open boundaries (e.g., Van der Wegen and Roelvink, 2008). When only the ebb delta is modeled, the modeled entrance is shallower than observed ones since their model used a fixed velocity profile in the entrance and hence no dynamic interaction between the tidal basin and the ebb delta (Van der Vegt et al., 2009; 2006). The present study views the tidal basin, entrance and tidal deltas as an integrated system. As a result, almost all morphological parameters have been reproduced. The analysis of the modeled hydrodynamics shows that profound changes in water depth, flood and ebb current velocities and durations have occurred at the entrance during the morphological evolution. The water and sediment exchanges between the basin and the open sea play an important role in the tidal inlet evolution.

Flood and ebb tidal deltas are important depositional features of tidal inlets. Their locations, spatial scales and deposition or erosion rates are changeable, controlled by many factors such as tidal prism, waves, river discharges, sediment sources and morphological development stages. As shown by FitzGerald et al. (2002), there are three sediment sources for the entrance channel, i.e., longshore drift, erosion from the bed of entrance, sediment from river; the amount of sediment supply will influence the spatial scales of tidal deltas. In this study, the flood delta is composed of several parts and much larger than the ebb delta. These characteristics are present in many natural environments, such as the Yuehu Lake in Shandong Peninsula, China (Jia et al., 2003) and Boao Harbor, Hainan Island, China (Gao et al., 2002). The probable reasons would be that the river discharge has an insignificant influence on the sediment supply to the ebb delta development and the intensity of longshore drift is relatively small.

5 Conclusions

In this paper, a numerical model is presented, which can be applied to simulate long-term evolutionary processes of tidal inlets. The model can reproduce almost all morphological elements of tidal inlet systems such as entrance channel, flood and ebb deltas, and secondary tidal channels. Morphodynamic equilibrium of the tidal inlet can be reached eventually, with a response time of the order of several years. The evolution rate of the tidal inlet system decreases with time exponentially, i.e., it is rapid at an earlier stage and slows down gradually. The mini-

mal cross-sectional area at the entrance enlarges with time, which agrees to the value calculated by the P-A relationship for the tidal inlets along East China coast when equilibrium is reached.

Negative feedback mechanisms exist between flow and bathymetric changes. Converging flood currents and jetting ebb currents are the main hydrodynamic mechanism for the formation of the entrance channel and flood/ebb deltas, whilst sediment transport is the central process in morphodynamic evolution which links tidal currents and morphological changes. The system tends to evolve towards morphodynamic equilibrium by adjusting water depth, flood and ebb current velocities and durations. The water and sediment exchanges between the basin and the open sea are important in the tidal inlet evolution. There exists nonlinear interaction among all the morphological elements of the system.

The physical mechanisms for the formation of multi-channel systems over the flood delta in the tidal basin are attributed to the action of both flood and ebb currents. At an earlier stage, the flood delta becomes progressively shallower, the current velocities are increased gradually, and the erosion is intensified accordingly. After the threshold of initial sediment motion is reached, the currents are able to erode the bed and channels are formed and developed.

Acknowledgements

The authors wish to thank Dr. Zheng Bing Wang (Deltares & Delft University of Technology, the Netherlands) for his valuable comments and suggestions. Sincere thanks are extended to the anonymous reviewers for their critical comments on the original version of the manuscript.

References

- Bertin X, Chaumillon E, Weber N. 2004. Morphological evolution and time-varying bedrock control of main channel at a mixed energy tidal inlet: Mauthusson inlet, France. *Marine Geology*, 204: 187–202
- Bruun P. 1978. *Stability of tidal inlets-theory and engineering*. Amsterdam: Elsevier, 507
- De Vriend H J, Capobianco M, Chesher T, et al. 1993. Approaches to long-term modeling of coastal morphology: a review. *Coastal Engineering*, 21: 225–269
- ECCHE (Editorial Committee for Chinese Harbors and Embayments). 1992. *Chinese Harbours and Embayments (Part V) (in Chinese)*. Beijing: China Ocean Press

- Eguiluz A, Wong K C. 2005. Second order tidally induced flow in the inlet of a coastal lagoon. *Estuarine, Coastal Shelf Science*, 64: 509–518
- Englund F, Hansen E A. 1967. Monograph on sediment transport in alluvial streams. Copenhagen: Teknisk Forlag, 1–62
- FitzGerald D M, Buynevich I V, Davis R A Jr, et al. 2002. New England tidal inlets with special reference to riverine-associated inlet system. *Geomorphology*, 48: 179–208
- Fletcher C A. 1988. Computational techniques for fluid dynamics. Berlin: Springer
- Gao Shu. 1988. P-A relationships of tidal inlets along the East China Sea coast. *Marine Science (in Chinese)*, (1): 15–19
- Gao Shu, Collins M B. 1994. Tidal inlet stability in response to hydrodynamic and sediment dynamic conditions. *Coastal Engineering*, 23: 61–80
- Gao Shu, Collins M B. 1998. Equilibrium coastal profiles: I. Review and synthesis. *Chinese Journal of Oceanology and Limnology*, 16(2): 97–107
- Gao Jianhua, Gao Shu, Chen Peng, et al. 2002. Long-shore sediment transport along the coast of Boao Harbour, Hainan Island, China. *Marine Geology & Quaternary Geology (in Chinese)*, 22(2): 41–48
- Gong Wenping, Shen Jian, Jia Jianjun. 2009. Feedback between tidal hydrodynamics and morphological changes induced by natural process and human interventions in a wave-dominated tidal inlet: Xiaohai, Hainan, China. *Acta Oceanologica Sinica*, 28(3): 93–113
- Gong Wenping, Shen Jian, Wang Daoru. 2008. Mean water level setup/set down in the inlet-lagoon system induced by tidal action—a case study of Xincun Inlet, Hainan Island in China. *Acta Oceanologica Sinica*, 27(5): 63–80
- Guyondet T, Koutitonsky V G. 2008. Tidal and residual circulations in coupled restricted and leaky lagoons. *Estuarine, Coastal Shelf Science*, 77: 396–408
- Hayes M O. 1975. Morphology and sand accumulation in estuaries. In: Cronin L E, ed. *Estuarine Research*. New York: Academic Press, 2: 183–200
- Hayes M O. 1980. General morphology and sediment patterns in tidal inlets. *Sedimentary Geology*, 26: 139–156
- Hibma A, Schuttelaars H M, De Vriend H J. 2004. Initial formation and long-term evolution of channel-shoal patterns. *Continental Shelf Research*, 24: 1637–1650
- Jarret J T. 1976. Tidal prism-inlet relationships. GITI report no. 3. Coastal Engineering and Research Centre, US Army Corps of Engineers, Fort Belvoir, VA
- Jia Jianjun, Gao Shu. 2008. A sedimentological approach to P-A relationships for tidal inlet systems: an example from Yuehu Inlet, Shandong Peninsula, China. *Frontiers of Earth Science in China*, 2(3), 262–268
- Jia Jianjun, Gao Shu, Xue Yunchuan. 2003. Sediment dynamics of small tidal inlets: An example from Yuehu inlet, Shandong Peninsula, China. *Estuarine, Coastal Shelf Science*, 57: 783–801
- Kragtwijk N G, Zitman T J, Stive M J F, et al. 2004. Morphological response of tidal basins to human interventions. *Coastal Engineering*, 51: 207–221
- Kraus N C. 1998. Inlet cross-sectional area calculated by process-based model. *Coastal Engineering*, 32: 65–3278
- Lanzoni S, Seminara G. 2002. Long-term evolution and morphodynamic equilibrium of tidal channels. *Journal of Geophysical Research*, 107, C1, 10.1029/2000JC000468
- Lesser G R, Roelvink J A, Van Kester J A, et al. 2004. Development and validation of a three-dimensional morphological model. *Coastal Engineering*, 51(8-9): 883–915
- Li Chunyan. 2002. Axial convergence fronts in a barotropic tidal inlet sand shoal inlet, VA. *Continental Shelf Research*, 22: 2633–2653
- O'Brien M P. 1931. Estuary tidal prism related to entrance areas. *Civil Engineering*, 1(8): 738–739
- O'Brien M P. 1969. Equilibrium flow areas of inlets on sandy coasts. *Journal of Water and Harbor Division*, 95(WW1): 43–52
- Ren Mei'E, Zhang Renshun. 1985. On tidal inlets of China. *Acta Oceanologica Sinica*, 3: 423–432
- Roelvink J A. 2006. Coastal morphodynamic evolution techniques. *Coastal Engineering*, 53: 277–287
- Roelvink J A, Van Banning G K. 1994. Design and development of DELFT3D and application to coastal morphodynamics. In: Babovic & Maksimovic, ed. *Hydroinformatics*. Rotterdam: Balkema, 451–456
- Stive M J F, Wang Zhengbing. 2003. Morphodynamic modeling of tidal basins and coastal inlets. In: Lakhan V C, ed. *Advances in Coastal Modeling*. Amsterdam: Elsevier, 367–392
- Van der Vegt M, Schuttelaars H M, De Swart H E. 2006. Modeling the equilibrium of tide-dominated ebb-tidal deltas. *Journal of Geophysical Research*, 111: F02013
- Van der Vegt M, Schuttelaars H M, De Swart H E. 2009. The influence of tidal currents on the asymmetry of tide-dominated ebb-tidal deltas. *Continental Shelf Research*, 29(1): 159–174
- Van der Wegen M, Roelvink J A. 2008. Long-term morphodynamic evolution of a tidal embayment using a two-dimensional, process-based model. *Journal of Geophysical Research*, 113: C03016

- Van Leeuwen S M, De Swart H E. 2002. Intermediate modelling of tidal inlet systems: Spatial asymmetries in flow and mean sediment transport. *Continental Shelf Research*, 22: 1795–1810
- Van Leeuwen S M, Van der Vegt M, De Swart H E. 2003. Morphodynamics of ebb-tidal deltas: a model approach. *Estuarine, Coastal and Shelf Science*, 57: 899–907
- Van Rijn L C. 1984. Sediment transport. Part II: Suspended load transport. *Journal of Hydraulic Engineering*, 110: 1613–1641
- Van Rijn L C. 1993. *Principles of Sediment Transport in Rivers, Estuaries and Coastal Seas*. Amsterdam: Aqua Publications
- Vila-Concejo A, Ferreira O, Matias A, et al. 2003. The first two years of an inlet: sedimentary dynamics. *Continental Shelf Research*, 23: 1425–1445
- Walton T L, Adams W D. 1976. Capacity of inlet outer bars to store sand. *Proceeding of 15th Coastal Engineering Conference*, Honolulu, ASCE, New York, 1919–1937
- Wang Zhengbing, Jeuken C, De Vriend H J. 1999. Tidal Asymmetry and Residual Sediment Transport in Estuaries. A Literature Study and Applications to the Western Scheldt, WL|Delft Hydraulics Report Z2749. Delft, the Netherlands
- Wang Zhengbing, Louters T, de Vriend H J. 1995. Morphodynamic modeling of a tidal inlet in the Wadden sea. *Marine Geology*, 126: 289–300
- Xie Dongfeng, Gao Shu, Wang Yaping. 2008. Morphodynamic modelling of open-sea tidal channels eroded into a sandy seabed, with reference to the channel systems on the China coast. *Geo-Marine Letters*, 28(4): 255–263
- Xie Dongfeng, Wang Zhengbing, Gao Shu, et al. 2009. Modeling the tidal channel morphodynamics in a macro-tidal embayment, Hangzhou Bay, China. *Continental Shelf Research*, 29(15): 1757–1767
- Zhang Qiaomin. 1987. On P-A relationships of tidal inlets along south China coast. *Journal of Tropic Oceanography*, 6(2): 10–18
- Zhang Renshun. 1995a. Tidal prism-throat area relationships of tidal inlets along Yellow Sea and Bohai Sea coast. *The Ocean Engineering (in Chinese)*, (2): 54–61
- Zhang Renshun. 1995b. Development of tidal inlet in mud coast along Bohai Bay. *Acta Geographica Sinica (in Chinese)*, 50(6): 506–513
- Zhang Qiaomin, Chen Xinshu, Wang Wenjie, et al. 1995. Geomorphological evolution of the entrances of the sandbar-lagoon type tidal inlets along the southern China coastlines. *Acta Oceanologica Sinica (in Chinese)*, 17(2): 69–77